

Zn(II)-Mediated Gold Nanosensors for Protein Phosphatase Assay

Jin Oh Lee,* Gae Baik Kim* and Young-Pil Kim*

*Department of Life Science, Hanyang University, Seoul 133-791, Republic of Korea,
ypilkim@hanyang.ac.kr

ABSTRACT

Protein phosphatases (PPs) have served as key molecules in a myriad of biological events. Since gold nanoparticle (AuNP)-based colorimetric assays have been preferred for enzyme activity assay, a few of attempts have been designed for the simple and rapid detection of PP activity. Here we report a simple AuNP colorimetric assay of PP activity using hexahistidine-tagged phosphopeptides and divalent metal ions, which does not require antibody and rare chemical. Among metal ions including nickel (II), copper(II), cobalt(II), magnesium (II), manganese (II), and zinc(II), only zinc (II) triggered self-assembly of AuNPs in the presence of hexahistidine-tagged phosphopeptides. In contrast, PP1 caused dephosphorylation of peptides, leading to no change in the color of the AuNP solution. As a result, the PP activity was easily quantified by the extinction ratio (E520/E700) of the colloidal gold assembly, where there was a linear correlation between the PP concentration and the extinction ratio. Most importantly, this method was successfully used for analyzing protein phosphatase 2A (PP2A) activity in immunoprecipitated plant extracts. Based on the results, we anticipate that our method will find the applications to monitor the activities of various PPs and their inhibition in a rapid format.

Keywords: gold nanoparticle, protein phosphatase, metal affinity, colorimetric assay, peptides, zinc coordination

1 INTRODUCTION

Protein phosphatases (PPs) are one of the most essential enzymes underlying the regulation of many cellular functions in a coordinated manner with protein kinases [1, 2]. To this end, many methods based on radioactive, chromogenic and fluorogenic detection have been developed to analyze to PP activity [3-5]. However, in addition to labor-intensive radioactive method, non-radioactive methods still suffer from high background signal, due to interfering substances or acidic reaction conditions. This is often restricted in a rapid read-out with high detection sensitivity.

To circumvent this limitation, we demonstrate herein a gold nanoparticle (AuNP)-based colorimetric sensor for the detection of PP activity using peptide substrate and metal ion affinity. While AuNP-based colorimetric assays have attracted attention in recent years, because of the high extinction coefficient of AuNPs and detection simplicity, only a few attempts have been made to assay PP activity

using AuNP-based colorimetry [6-8]. Unlike the AuNP-based assay based on simple electrostatic interactions between phosphorylated and dephosphorylated peptides, the designed AuNP nanosensor provides highly reliable detection of dephosphorylated products via a strong metal-coordinated affinity. The rationale stems from structural information of the conserved active site of common PPs, where two metal ions generally coordinates with a phosphate group of a substrate by three histidines, two aspartic acids, and one asparagine in the binding pocket [9]. Being inspired by this principle, we employed nitrilotriacetic acid (NTA)-modified AuNPs and histidine-tethered phosphopeptide to induce the metal coordination. In the present study, we investigated metal specificity and effects of metal ion concentration and pH condition on the self-assembly of AuNPs. PP activity was also investigated in plant extract to verify the usability of this nanosensor.

2 EXPERIMENTAL

2.1 Synthesis of NTA-AuNPs

To generate NTA-AuNPs, 40 mg of carboxymethyl-polyethylene glycol-thiol (CM-PEG-SH, MW=3,400, Laysan Bio, Inc) was added to the citrate-stabilized AuNP solution (20 mL at 12 nM), followed by vigorous stirring at RT. The carboxy AuNP was further modified with N α ,N α -bis(carboxymethyl)-L-lysinehydrate (NH₂-NTA, Sigma) via EDC. The molar concentration of NTA-AuNP was calculated by dividing the total number of gold atoms by the average number of gold atoms per AuNP after confirming the size.

2.2 AuNP-Based Colorimetric Analysis

Unless otherwise stated, NTA-AuNPs (2.5 μ L at 250 nM), peptide substrate (2.5 μ L at 100 μ M), and divalent ion (10 μ L at 10 mM) were mixed to give a final volume of 100 μ L in 20 mM Tris-HCl buffer (pH 7.4) and incubated at RT for 1 h, after which extinction spectra were measured using a plate reader (VarioskanTM Flash, Thermo Scientific). The peptide substrates (His₆-pPep; H₆GLRRASpLG, His₆-Pep; H₆GLRRASLG, and pPep; GLRRASpLG) were synthesized by Peptron Inc., Korea. For the divalent ion experiments, NiCl₂, CoCl₂, CuCl₂, MnCl₂, MgCl₂, or ZnCl₂ was added to the reaction mixture at a final concentration of 1 mM.

2.3 Protein Phosphatase Assay

Protein phosphatase 1 (PP1, New England Biolabs) (5 μL at different concentrations) was incubated at 30 $^{\circ}\text{C}$ for 1 h with peptide substrate (2.5 μL at 100 μM) and MnCl_2 (5 μL at 10 mM) in the reaction buffer (20 mM Tris-HCl, pH 7.4). For the AuNP-based assay, the reactant was transferred to 96-well plate and further mixed with NTA-AuNPs (2 μL at 250 nM) and ZnCl_2 (10 μL at 10 mM) at RT to give a final volume of 100 μL in 20 mM Tris-HCl buffer (pH 7.4). After completing the reaction at RT for 1 h, the extinction of the solution was determined using a plate reader.

2.4 Protein Phosphatase Assay in Plant Extracts

Protein extracts from wild-type Columbia-0 (Col-0) or transgenic *Arabidopsis thaliana* that expressed PP2A-A1 were prepared in extraction buffer (50 mM Tris-HCl, pH 7.5, 50 mM NaCl, 300 mM sucrose, 1% Triton X-100, 0.2 mM PMSF and 1 \times protease inhibitor cocktail). For immunoprecipitation (IP), soluble supernatant from protein extracts was incubated for 75 min with protein A agarose bead (Thermo Scientific Inc.) conjugated with polyclonal anti-PP2A1 tag (YFP) antibody (homemade, 4.6 μg μL^{-1}). For the AuNP-based assay, immunoprecipitated proteins from wild-type and PP2A-A1-expressed fractions were washed four times with extraction buffer and then incubated with His₆-pPep substrate (2.5 μL at 100 μM) in the presence of MnCl_2 (5 μL at 10 mM) dissolved in reaction buffer (20 mM Tris-HCl buffer, pH 7.4) at RT for 1 h with vigorous shaking. Aliquots (50 μL) of the reaction mixture were transferred to 96-well plates and were mixed with NTA-AuNP and ZnCl_2 . After additional incubation at RT for 1 h, the extinction of the mixture was measured using a plate reader.

3 RESULTS AND DISCUSSION

As illustrated in Fig. 1, we hypothesized that NTA-AuNPs (21.3 \pm 1.1 nm in core diameter) can be bound strongly to the hexahistidine and phosphate group of His₆-tagged phosphopeptide (His₆-pPep: H₆GLRRASpLG) via Zn(II) coordination because Zn(II)-chelated ligand (NTA) is known to have strong affinity for hexahistidine [10, 11] and phosphate group [12-14]. This cross-link brings about the self-assembly of NTA-AuNPs, resulting in a color change from reddish-brown to violet. In contrast, dephosphorylation of peptide substrates by PP activity could not cause the cross-link of NTA-AuNPs, due to lack of Zn(II)-phosphate coordination.

To check this possibility, different divalent ions including Ni(II), Co(II), Cu(II), Mn(II), Mg(II), and Zn(II) were tested in the presence of His₆-pPep and NTA-AuNPs (Figure 2). Among the tested divalent ions, only Zn(II) induced self-assembly of NTA-AuNP, resulting in changes in extinction and color from reddish-brown to reddish-violet (Figs 2A and 2B), whereas other divalent ions did

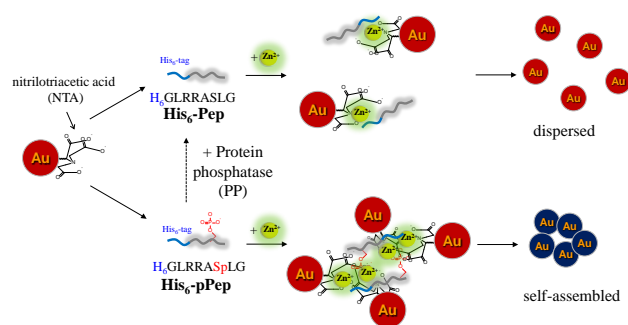


Figure 1: Schematic of colorimetric PP activity assay using NTA-modified AuNPs and His₆-tagged phosphopeptides (His₆-pPep) in the presence of Zn^{2+} . The PP activity inhibits the assembly of NTA-AuNPs by dephosphorylation of His₆-pPep (top right), whereas NTA-AuNPs are self-assembled by Zn^{2+} -coordination (bottom right).

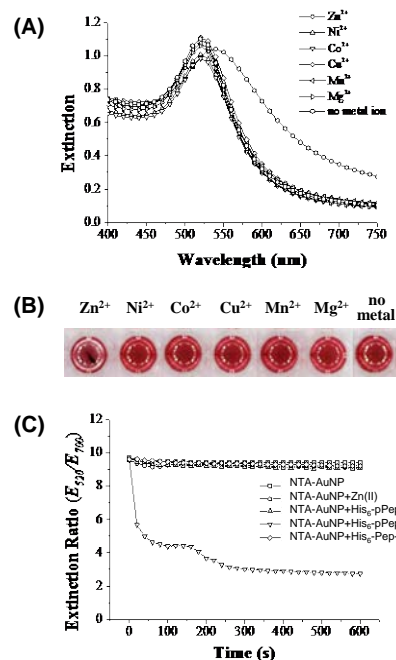


Figure 2: Effect of different divalent ions on the self-assembly of NTA-AuNPs with His₆-pPep (H₆GLRRAS(p)LG) in (A), (B), and (C) or His₆-Pep (H₆GLRRASLG) in (C): (A) extinction spectra, (B) photograph of the NTA-AuNP solutions, and (C) time-lapse changes in the extinction ratio (E_{520}/E_{700}) of NTA-AuNPs.

The final concentrations of NTA-AuNP, peptide, and divalent ion were 5 nM, 2.5 μM , and 1 mM, respectively.

not give rise to a significant color change at the same concentrations. Importantly, time-lapse extinction graph showed that Zn(II)-induced self-assembly rapidly occurred approximately 5 min after the addition of Zn(II) ions (Fig. 2C).

To examine whether the Zn(II)-mediated self-assembly of NTA-AuNPs is induced by His₆-pPep, different synthetic

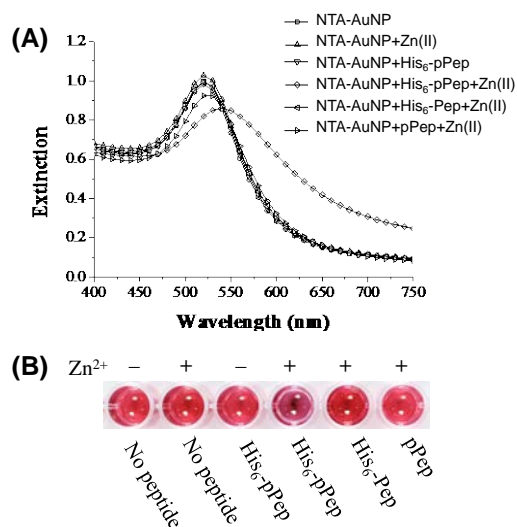


Figure 3: (A) Extinction spectra and (B) photograph of NTA-AuNPs in the presence and absence of Zn²⁺ with different peptides (His₆-pPep, His₆-Pep, and pPep (GLRRAS(p)LG).

peptides (His₆-Pep; H₆GLRRASLG and pPep; GLRRAS(p)LG) were tested. In Fig. 3, while the original color of NTA-AuNPs was not affected by addition of either Zn(II) or His₆-pPep, significant self-assembly of NTA-AuNPs was only observed in the presence of both His₆-pPep and Zn(II). There was no color change when unphosphorylated peptide (His₆-Pep) or His₆-deficient peptide (pPep) was used under the same conditions. Although the coordination structure is not clearly understood in this study, these results strongly support that Zn(II) can provide better binding affinity for both a substrate P-O⁻ group and a His₆-tag than other metal ions. Consequently, the self-assembly of NTA-AuNPs in the presence of Zn(II) discriminated phosphorylation of histagged peptides.

To assay protein phosphatase activity using this AuNP-based colorimetry, extinction of NTA-AuNPs was monitored as a function of protein phosphatase 1 (PP1) concentrations in the presence of His₆-pPep and Zn(II). In Figs 4A and 4B, there was a linear correlation between the extinction ratio and PP1 concentration in the range of 0.05 U to 0.5 U. The maximal recovery yield was 83.5 % at 5 U PP1, based on the relative extinction ratio of His₆-Pep (control). Most importantly, bovine serum albumin (BSA), of which concentrations were equivalent to those of full active PP1, caused a negligible change under the same conditions (Fig. 4C). When the extinction ratio was converted to the activity level (%), a critical difference in activity level was observed between PP1 and BSA (Fig. 4D), indicating that the self-assembly of NTA-AuNPs/Zn(II) in the presence of pep1 is controlled by the enzymatic activity of PP1. The detection sensitivity for PP1 in Fig. 4A was as low as 0.01 U, which is greater than that

0.4 U of the traditional colorimetric assay using *p*-nitrophenyl phosphate [15].

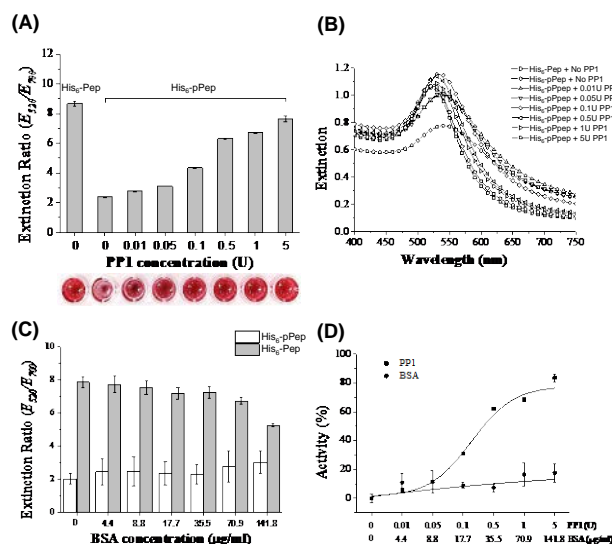


Figure 4: Colorimetric assay of protein phosphatase 1 (PP1) activity using NTA-AuNP and His₆-pPep in the presence of Zn²⁺. Changes in (A) extinction ratio and (B) extinction spectra of the NTA-AuNP solution were displayed as a function of PP1 concentration, ranging from 0.01 to 5 U. (C) Control experiment as a function of bovine serum albumin (BSA) concentration. (D) The activities from PP1 and BSA were calculated and plotted from the extinction ratios.

To further investigate whether this method is useful for analyzing PP activity in real samples, PP activity from plant extracts was measured using this gold nanosensors (Fig. 5). Total proteins was initially extracted from transgenic *Arabidopsis thaliana* overexpressing PP2A-A1 (one of three isoforms of PP2A) fused to YFP and wild-type *A. thaliana* (Columbia-0, abbreviated Col-0), which was followed by enrichment by immunoprecipitation (IP) using anti-PP2A tag polyclonal antibody (anti-YFP pAb) attached to the protein A agarose beads (Fig. 5A). When each aliquot of immunoprecipitated beads was incubated with His₆-pPep and NTA-AuNP/Zn(II) in a microwell plate (Fig. 5B), a relatively higher recovery of the color of NTA-AuNPs, which was responsible for PP2A activity, was observed in immunoprecipitated proteins obtained from transgenic PP2A extracts than wild-type (Fig. 5C). Compared to the control (the first well in Fig. 5C), an increased level of PP2A activity was detectable in wild-type extracts, probably due to endogenous PP2A. This result indicates that IP-combined colorimetric detection would be very useful for *in vitro* analysis of PP activity in complex samples.

Despite the reversible sensing ability to phosphorylation, our colorimetric format was limited to detect protein kinase activity, because abundant adenosine triphosphates in a reaction buffer of protein kinase critically impeded the

phosphopeptide-Zn(II) interaction on the NTA-AuNP (data not shown). Therefore, the assay format described in this paper is more suitable for measuring PP activity, than protein kinase activity.

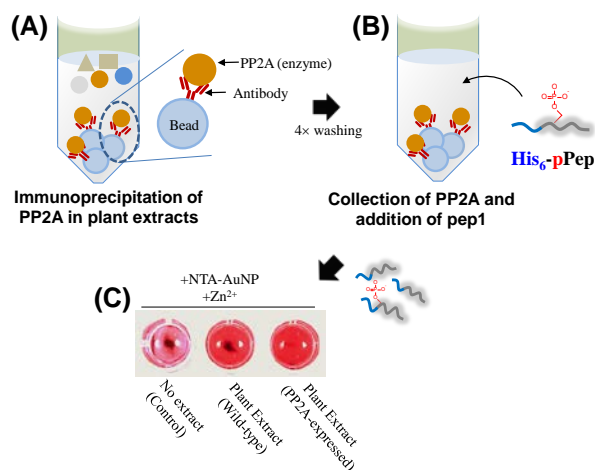


Figure 5: Immunoprecipitation (IP)-combined colorimetric assay of PP2A activity in plant extracts using NTA-AuNPs: (A) IP of PP2A using anti-PP2A-tag antibody and (B) PP2A reaction with His₆-pPep after IP. (C) Photographs of NTA-AuNPs on PP2A activity in control (free extract), extract (wild-type Col-0), and transformant extract (PP2A-expressed).

Due to their high surface-to-volume ratio, NTA-AuNPs were self-assembled rapidly via strong binding affinity with Zn(II) ions in the presence of His₆-tagged phosphopeptides, which would not be possible using other NTA-coated beads or metal-chelating microparticles.

4 CONCLUSIONS

We reported the simple and rapid detection of PP activity using Zn(II)-mediated colorimetric gold nanosensors with His₆-tagged phosphopeptides. As a result of specific Zn(II)-coordination between the carboxy groups of NTA-AuNPs and the oligohistidine and phosphate groups of His₆-tagged phosphopeptides, the self-assembly of NTA-AuNPs was controlled by PP1 activity-driven dephosphorylation, which allowed for the quantification PP activity based on the extinction ratio (E_{520}/E_{700}) of NTA-AuNP. Furthermore, the gold nanosensor combined with IP was capable of detecting PP2A activity in plant extracts. We anticipate that our method will be useful for studying the physiological activities of PPs in a simple and rapid manner.

ACKNOWLEDGMENTS

This work was supported by Mid-career Researcher Program (No. 2013R1A2A2A03015161) and

Nano-Material Technology Development Program (No. 2012M3A7B4035286) through the National Research Foundation (NRF) funded by the Ministry of Science, ICT, and Future Planning (MSIP).

REFERENCES

- [1] A. L. Bauman, and J. D. Scott, *Nat. Cell Biol.*, 4, E203-E206, 2002.
- [2] A. Bononi, C. Agnoletto, E. De Marchi, S. Marchi, S. Patergnani, M. Bonora, *et al.*, *Enzym. Res.*, 329098, 2011.
- [3] T. McAvoy and A. C. Nairn, "Serine/threonine protein phosphatase assays. Current protocols in molecular biology" edited by Frederick M Ausubel [et al] Ch. 18, Unit18, 2010.
- [4] U. Lorenz, "Protein tyrosine phosphatase assays. Current protocols in immunology" edited by John E Coligan [et al], Ch 11, Unit 11, 2011.
- [5] M. Brune, J. L. Hunter, J. E. Corrie, and M. R. Webb, *Biochemistry*, 33, 8262-8271, 1994
- [6] Y. Choi, N. H. Ho, and C. H. Tung, *Angew. Chem. Int. Ed.*, 46, 707-709, 2007..
- [7] T. Serizawa, Y. Hira, and M. Aizawa, *Mol. BioSys.*, 6, 1565-1568, 2010.
- [8] J. Zhou, X. Xu, X. Liu, H. Li, Z. Nie, M. Qing, et al., *Biosens. Bioelectron.*, 53, 295-300, 2014.
- [9] Y. Shi, *Cell*, 139, 468-484, 2009.
- [10] S. Y. Park, S. M. Lee, G. B. Kim, and Y. P. Kim, *Gold Bull.*, 45, 213-219, 2012.
- [11] G. B. Kim, K. H. Kim, Y. H. Park, S. Ko, and Y. P. Kim, *Biosens. Bioelectron.* 41, 833-839, 2013.
- [12] E. Kimura, *Pure Appl. Chem.*, 65, 355-359, 1993.
- [13] E. Boby, J. K. Lassila, H. I. Wiersma-Koch, T. D. Fenn, J. J. Lee, I. Nikolic-Hughes, et al., *J. Mol. Biol.*, 415, 102-117, 2012.
- [14] T. H. Evers, M. A. M. Appelhof, F. W. Meijer, and M. Merckx, *Protein Eng. Des. Sel.*, 21, 529-536, 2008.
- [15] H. Sotoud, P. Gribbon, B. Ellinger, J. Reinshagen, P. Boknik, K. Kattner, et al., *J. Biomol. Screen*, 18, 899-909, 2013.